Microchimica Acta (2018) 185: 194
https://doi.org/10.1007/s00604-018-2715-8

ORIGINAL PAPER

Amperometric determination of nitrite using natural fibers as template for titanium dioxide nanotubes with immobilized hemin as electron transfer mediator

Balasubramanian Ranjani[1] · Jayaprakasham Kalaiyarasi[1] · Loganathan Pavithra[2] · Thiyagarajan Devasena[2] · Kannaiyan Pandian[1] · Subash C. B. Gopinath[3,4]

Received: 24 November 2017 / Accepted: 26 January 2018 / Published online: 23 February 2018

Abstract

A sensing device was constructed for the amperometric determination of nitrite. It is based on the use of titanium dioxide (TiO_2) nanotubes template with natural fibers and carrying hemin acting as the electron mediator. A glassy carbon electrode (GCE) was modified with the hemin/TNT nanocomposite. The electrochemical response to nitrite was characterized by impedance spectroscopy and cyclic voltammetry. An amperometric study, performed at a working potential of + 0.75 V (vs. Ag/AgCl), showed the sensor to enable determination of nitrite with a linear response in the 0.6 to 130 μM concentration range and with a 59 nM limit of detection. Corresponding studies by differential study voltammetry (E_p = 0.75 V) exhibited a linear range from 0.6×10^{-6} to 7.3×10^{-5} M with a limit of detection of 84 nM. The sensing device was applied to the determination of nitrite in spiked tap and lake water samples.

Keywords Kenaf fiber · Nanocomposites · Electrocatalytic oxidation · Limit of detection · Water samples

Introduction

Nitrite is being widely used in meat curing [1], food preservatives [2], dyes and bleaches [3], fertilizers as well as for medicinal purposes. Numerous health hazards like Methemoglobinemia or "blue baby syndrome", gastric cancer [4], spontaneous intrauterine growth restriction [5], abortions and birth defects have been associated with high nitrite concentrations. The relative standard has been established to limit the concentration of nitrite in aquaculture and drinking water because of the damages held by their higher concentration. The World Health Organization (WHO) set the safe limit of nitrite in potable water is 3 mg/L [6]. The generation of portable and cheap sensors with high sensitivity and selectivity is considered to be a challenge. Nitrite from environment and food sources can react with amine groups to yield carcinogenic agent nitrosamines [7]. Because of the occurrence of toxicity in biological system there is a need to monitor the level of nitrite concentration accurately; many strategies have been demonstrated for the efficient analysis of nitrite, which includes ion-chromatography [8], spectroscopic method [9], chemiluminescence [10], spectrofluorimetry [11] and electrochemical method [12]. Among these strategies, electrochemical method is a promising high performance tool with an excellent advantage of reliability, high sensitivity and good selectivity. Nevertheless, the estimation of nitrite on bare glassy carbon electrode (GCE), has limitations due to several species that can poison the surface of the electrode [13]. To overcome this issue, electrodes were chemically modified and used. The aim of the chemical modification on the electrode surface is to avoid electrode fouling and to enhance the electrocatalytic oxidation of nitrite [14]. Various redox mediators modified nanomaterials and conducting polymer based sensors have

Electronic supplementary material The online version of this article (https://doi.org/10.1007/s00604-018-2715-8) contains supplementary material, which is available to authorized users.

✉ Kannaiyan Pandian
jeevapandian@yahoo.co.uk

[1] Department of Inorganic Chemistry, University of Madras, Guindy Campus, Chennai 600025, India

[2] Centre for Nanoscience and Technology, Anna University, Chennai 600025, India

[3] School of Bioprocess Engineering, Universiti Malaysia Perlis, 02600 Arau, Perlis, Malaysia

[4] Institute of Nano Electronic Engineering, Universiti Malaysia Perlis, 01000 Kangar, Perlis, Malaysia

been widely utilized for the sensitive high performance analysis of nitrite. For instant the modification on the electrode such as chit/Prussian blue nanoparticles modified on a mixture of graphene nanosheets and carbon nanospheres [15], poly(3,4-ethylenedioxythiopene) / iron phthalocyanine / multi-walled carbon nanotubes (PEDOT/FePc/MWCNTs) [16], gold/reduced graphene oxide/poly (diallyldimethylammonium chloride) (Au-rGO/PDDA) [17], multilayer of carboxylated nanocrystalline cellulose and PDDA in PEDOT host [18], AuNC/PEDOT [19], thionine modified CNTs [20], rGO modified GCE [21], titanium dioxide nanoparticles/ionic liquid composite electrode [3], rGO/MWCNTs [22], polyaniline/MoS_2 nanocomposites [23], rGO/ferrocene [24], PEDOT/PAS [25], Cobalt nanostructures /GO/PPy) [26], and nano-sized hydroxyapatite/PEDOT [27] have shown lower detection limits towards electrochemical detection of nitrite in various samples.

Metal oxides are attracted for the purpose of fabrication and ultimate use in making sensing devices, due to their attested advantages with the production flexibility, low cost, and good thermal and chemical stability [28]. Because of the high surface area, TNT has been widely used as substrate to immobilize various redox active molecules and enzymes for fabrication of drug delivery vehicle and biosensors [29], electrocatalysis [30] and solar cell devices [31]. Mostly, TNT can be synthesized by template-assisted method using porous alumina (AAO) [32], electrochemical etching of titanium foil [33] and hydrothermal method [34]. Imai et al. [33, 35] and other have exploited natural fibers as a template to prepare using various titanium salt precursors [36]. However, Imai et al. have shown the stepwise precipitation of TiF_4 on glass, cotton fiber, and porous alumina in acid pH range yield a thin coating of the anatase form of TNT.

Natural fibers have gained attention in the manufacturing of various metal oxide based nanostructures. Hence, natural fibers like kenaf, jute, sisal, hemp, and bamboo are widely used as template to prepare metal oxides [37]. We have shown that linen fibers can be used for the preparation of a regular shaped titanium oxide which was used to immobilize the metal nanoparticles and another catalyst [36]. Herein, we attempted to use kenaf (*Hibiscus cannabinus L.*) as a template to prepare uniform sized titanium oxide nanoparticles after purification with alkali treatment. Kenaf fiber (KF) is cheap, contains low-density materials, cellulose-rich fiber and possesses good mechanical properties [38]. Generally, kenaf fiber length is 1 to 5 mm and its diameter was 0.5 to 2 mm. In the current research, we generated an elegant method with hemin modified TNT based electrochemical sensor device to determine nitrite in water sources. Hemin is a generally accepted iron-containing porphyrin, a well-known active center of the heme-protein family such as CytC, hemoglobin, myoglobin, peroxidase etc. [39]. Hemin has been used as a cheap electron transfer mediator as it enhances various redox reactions at lower overvoltage ranges with stable redox system. It can be easily immobilized on solid supports through π-interaction onto graphene sheet and covalent modification on carbon fibers [40]. Hemin can be modified with TNT through a strong electrostatic attraction of two carboxylic acid functional group and also avoids the molecular aggregation in aqueous solution, improves the stability and enhance the activity of the catalyst because of free molecular self-assembly [41]. In the present investigation, we prepared a stable hemin tagged TNT for the enhanced electrochemical analysis of nitrite and results were comparable with the previous published papers. The present system showed an excellent sensitive and lower detection limit than the previous published results.

Experimental methods

Materials

Titanium tetrafluride (TiF_4), hemin, potassium chloride (KCl), and phosphate buffer reagents (Na_2HPO_4, NaH_2PO_4) were procured from Sigma-Aldrich (Biocorporals Pvt. Ltd., Chennai, India, http://www.biocorporals.net). Sodium nitrite was purchased from SRL (Vijaya Scientific, Chennai, India, http://www.vijayascientific.com). The solvents (ammonia, ethanol, and acetone) used belong to analytical grade procured from the commercial source (Sudagar biological and chemicals, Chennai, India, sbcbio.in/) and used as such without involving further steps for the purification. Kenaf fibers (length: 1–5 mm and diameter: 0.5 – 2 mm) were collected from the Textile Technology Department, Anna University as a gift sample.

A buffer with a pH of 7.0 was made by suspending 0.1 M KCl with 0.1 M NaH_2PO_4, and 0.1 M Na_2HPO_4 in 250 mL standard flask using DI water. The pH of the solution was adjusted by an Elico-pH meter (Elico, Pvt. Ltd., India, www.elico.co/) at room temperature. The stock solution of 0.1 M nitrite was prepared freshly with DI water and kept at 4 °C under conditions of the dark.

Instrumentation

Morphological and structural interpretation of the samples were analysed by field emission scanning electron microscopy (FE-SEM, SU6600, Hitachi, Japan) at an operating voltage of 15 kV. For this powdered sample XRD pattern was registered by XPERT-PRO diffractometer with a Cu-Kα_1 radiation (λ = 1.5406 Å). Confocal Raman spectroscopy model 11I, Nanophoton, Japan, with Ne-Ar laser (λ = 532.9 nm) and grating (600/mm) was used in recording Raman spectra. Bruker Vector-22 Fourier transform spectrometer was used to record Fourier transform infrared (FT-IR) spectrum at an ambient room temperature (RT) in attenuated total reflection mode

(ATR-FT-IR) in the wavenumber range of 400 – 4000 cm^{-1}. Thermal stability of the nanocomposite was monitored by thermogravimetric analysis (TGA) using a TGA Q5000, Thermal Analyzer (TA) instruments at a heating rate of 20°/min from room temperature up to 800 °C under the nitrogen atmosphere. Gamry (USA model 330) included with PV 220 software and a CHI 660B electrochemical system (CH instruments, Texas, USA) was used to carry out the electrochemical experiments. A single compartment electrochemical cell setup with 3 electrode system consisting of GCE (3 mm in diameter), platinum wire [0.5 mm in diameter and the Ag/AgCl (3 M KCl)] were used as a working, counter and reference electrodes respectively. Polishing kit was procured from BAS instruments (USA) to polish the GCE surface.

The modified electrode was investigated using cyclic voltammetry (potential window: - 0.6 V to +1.2 V, scan rate: 50 $mV{\cdot}s^{-1}$), chronoamperometry curve of nitrite oxidation was observed at a potential step of + 0.75 V for 60 s, Differential pulse voltammetry (Scan rate: 20 $mV{\cdot}s^{-1}$, Pulse width: 50 mV, Pulse amplitude: 25 mV), and amperometric (i-t) curves of nitrite were monitored at an supplied potential of + 0.75 V under hydrodynamic condition.

CHI-660B electrochemical system with supplying of AC voltage with 5 mV amplitude with a frequency ranges from 0.1 Hz to 100 kHz was used to carry out electrochemical impedance spectroscopy measurements. The redox probe was made by utilizing 10 mM $[Fe(CN)_6]^{3-/4-}$ having 0.1 M KCl in 250 mL standard flask using DI water. All the prepared solutions were exposed to high pure nitrogen gas for about 10 min before performing the electrochemical experiments.

Preparation of TiO_2 nanotubes

Kenaf plant fibers were finely cut and then precleaned with 1 M alcoholic KOH solution under ultrasonic irradiation to remove all organic impurities. Finally, the fibers were washed with DI water and subsequently washed with acetone. To deposit TiO_2 thin film onto finely cut plant fibers was placed in a 100 mL Teflon® beaker which contains 0.04 M of TiF_4 solution (pH of the solution was adjusted to 2 using 1% NH_4OH) and the temperature of the medium was fixed at 60 °C for 24 h in a hot air oven. The TiO_2 modified fibers were isolated by filtration and then dried under nitrogen atmosphere and finally calcined at 500 °C for 1 h in muffle furnace to remove the template.

Preparation of hemin/TNT nanocomposites

200 mg of hemin and 200 mg of TNT were taken for preparing hemin/TNT nanocomposites. Hemin was first dissolved in 20 mL of ethanol and then TNT was added and left stirring for 24 h to obtain a homogenous suspension of hemin/TNT nanocomposites. After 24 h, the reaction mixture was centrifuged at 2000 rpm for 15 min and then washed three times with DI water and acetone, thereafter dried overnight at 60 °C in a hot air oven.

Preparation of hemin/TNT/GCE

The hemin/TNT nanocomposites modified electrode was fabricated by the following procedure. The surface of GCE was first cleaned mechanically by polishing with alumina (0.5 μm powder) and thoroughly rinsed with DI water, followed by washing with 1:1 *v*/v ratio of nitric acid and eventually with DI water, dried at room temperature. About 1 mg of hemin/TNT nanocomposites was dispersed in 1 mL of ethanol and sonicated for 10 min. The colloidal suspension of hemin/TNT (5 μL) was drop casted onto the surface of GCE and allowed to dry at room temperature. The schematic diagram represents the surface modification process and electrochemical oxidation of nitrite corresponding to hemin/TNT/GCE.

Results and discussion

TNT is flexible to be prepared straightforwardly from natural resources and the resultant nanostructure possesses high surface area, good thermal and chemical stability. Since TNT can be prepared easily, the production cost is economical. Due to high surface area possessed by the TNT nanostructure, the electrochemical reaction kinetics will be good and owing to this reason, we prepared TNT from kenaf fibers for electrochemical sensing of nitrites.

Electrochemical behavior of the hemin/TNT modified electrodes

CV investigation of hemin/TNT modified GCE was examined utilizing potassium ferricyanide as an electrochemical probe. Figure 1a shows the CV curves of a) bare GCE, b) TNT/GCE, and c) hemin/TNT/GCE with 10 mM $K_3[Fe(CN)_6]^{3-/4-}$ having 0.1 M KCl at a scan speed of 50 $mV{\cdot}s^{-1}$ at different modified electrodes.

The CV of the modified electrodes depicted a pair of well-defined redox peaks representing $K_3[Fe(CN)_6]^{3-/4-}$ redox couple. Furthermore, the modified electrodes had more peak current and minimizing of peak separation was compared to bare GCE. The peak potential separation at the modified electrode lowered compared to bare GCE stating that the hemin/TNT significantly enhances the electron transfer process because of the increment in the surface area to volume ratio. The peak potential separation was calculated for the single electron transfer of Fe^{3+}/Fe^{2+} redox reaction at hemin/TNT modified electrode ($\Delta E_p = 68$ mV) which is 29 mV lower than that of bare GCE ($\Delta E_p = 97$ mV) is due to the negatively charged surface modified hemin/TNT, which repel the electron transfer

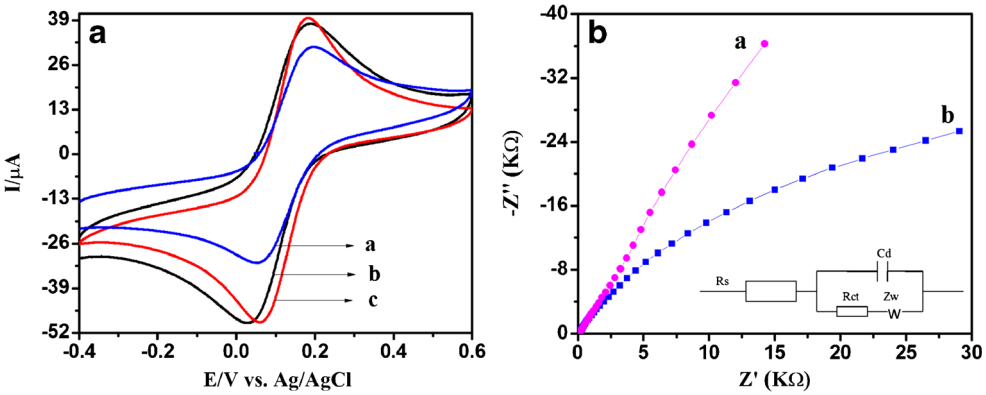

Fig. 1 **a** CV of a) bare GCE, b) TNT/GCE and, c) hemin/TNT/GCE in the presence of 10 mM $[Fe(CN)_6]^{3-/4}$ containing 0.1 M KCl at a scan rate of 50 mV·s^{-1}. **b** Nyquist plots of a) bare GCE, and b) hemin/TNT/GCE in the presence of 10 mM $[Fe(CN)_6]^{3-/4}$ containing 0.1 M KCl as the supporting electrolyte. AC Amplitude: 5 mV; Frequency range: 0.01 Hz to 100 kHz. Inset is the Randles circuit

reaction. On the other hand, significant enhancement in peak current value was noted in which the electron transfer of the probe is due to the hemin/TNT catalysis. It is inferred that the hemin/TNT system favors the electron transfer rate of the redox probe.

Electrochemical impedance spectroscopy (EIS)

Electrochemical behavior of hemin/TNT/GCE was investigated by EIS in 10 mM $[K_3Fe(CN)_6]^{3-/4-}$ containing 0.1 M KCl as supporting electrolyte in the frequency range of 0.1 Hz to 100 kHz with applying of 5 mV of AC signal amplitude. The semicircular portions of Nyquist plot at higher frequencies represent the electron transfer limited process and its diameter is equivalent to the electron transfer resistance (R_{ct}), which reflects electron transfer kinetics of redox probe on electrode-solution interface. Moreover, the linear part of Nyquist plot at low frequency corresponds to diffusion process and the semicircle diameter is equivalent to the charge transfer resistance (R_{ct}). From the Fig. 1b, displays the Nyquist plots for a) bare GCE that exhibits a straight line indicating the diffusion limited process whereas the hemin/TNT/GCE shows a small semi-circle in the high frequency region (curve b) is due to an interfacial electron transfer resistance (R_{ct}). The hemin/TNT exhibits an interfacial electron transfer resistance of 20 KΩ which hinder the electron transfer rate of $K_3[Fe(CN)_6]^{3-/4-}$. These results imply that hemin/TNT nanocomposites are successfully immobilized on GCE surface.

Electrocatalytic oxidation of nitrite at hemin/TNT modified GCE

The modified GCE was used for the electrochemical oxidation of nitrite in phosphate buffer (pH 7.0; containiing 0.1 M KCl). The CV behavior of nitrite on a) bare GCE, b) 3.3 × 10^{-4} M of nitrite on bare GCE, c) hemin/TNT modified GCE, and d) hemin/TNT in the presence of 3.3 × 10^{-4} M with buffer (pH 7.0) at a scan rate of 50 mV·s^{-1} as display in Fig. 2. A poor anodic oxidation peak was observed with an oxidation peak potential of + 0.75 V vs. Ag/AgCl whereas in the case of hemin/TNT/GCE a slight shifting of peak position was observed with a several fold enhanced oxidation peak current value than the bare GCE. The oxidation peak current values increase with increasing the concentration of nitrite in the linear range from 0.6 × 10^{-4} M to 7.3 × 10^{-3} M as indicated in Fig. 3a. The linear regression equation of $I_p = 23.6335$ C (mM) – 2.1862 with corresponding to a correlation coefficient of 0.9990 was attained as displayed in Fig. 3b.

Optimization of method

The following parameters such as (a) Buffer pH value; (b) Scan rate were optimized and its respective data and figures (Fig. S3 and Fig. S4) are given in the supporting

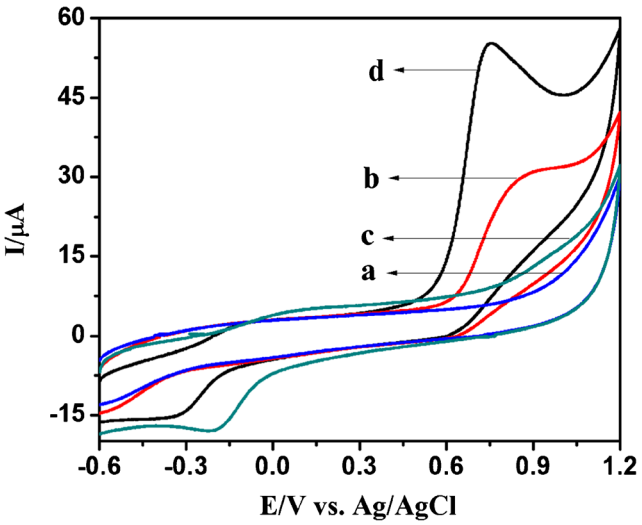

Fig. 2 Cyclic voltammograms of a) bare GCE, b) 3.3 × 10^{-4} M of nitrite on GCE, c) hemin/TNT modified bare GCE, and d) hemin/TNT/GCE in presence of 3.3 × 10^{-4} M with buffer (pH 7.0) of nitrite at scan rate of 50 mV·s^{-1} in 0.1 M buffer (pH 7.0) (d)

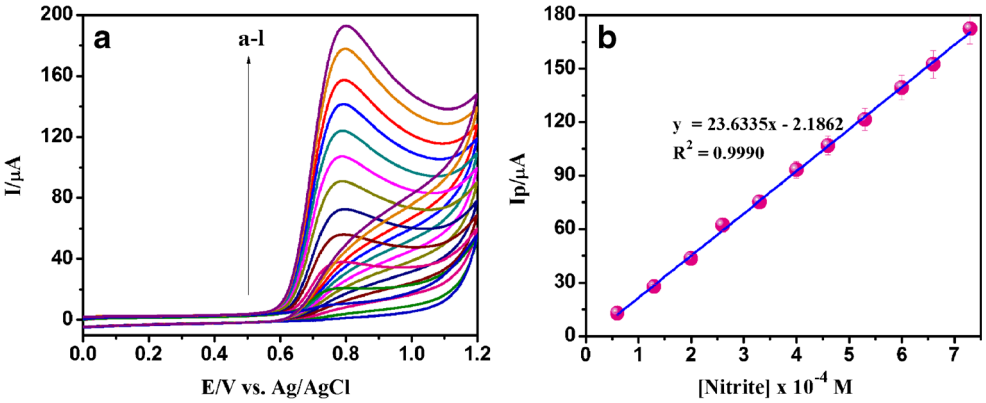

Fig. 3 Cyclic voltammograms of hemin/TNT/GCE with phosphate buffer (pH 7.0; containing 0.1 M KCl) for different concentrations ranging from 0.6×10^{-4} to 7.3×10^{-3} M of nitrite at a scan rate 50 mV·s^{-1} (**a**). Calibration plot of electrocatalytic peak current (I_{pa}) vs. conc. of nitrite (**b**)

information. The following experimental conditions were found to give best results: (a) Optimum buffer pH value: pH = 7.0; (b) Optimum scan rate: 50 mV·s^{-1}. Furthermore, the electrocatalytic oxidation of nitrite at the modified GCE exhibits that 2 electrons participate in the transfer process and is also discussed in the (supporting information).

Chronoamperometry studies

Chronoamperometry study was followed to find out the diffusion coefficient of nitrite oxidative process at hemin/TNT/GCE. Figure S5A displays the current-time relationships of hemin/TNT/GCE were attained by setting the working electrode potential of + 0.75 V vs. Ag/AgCl for nitrite at various concentrations of 0.05 to 0.2 mM in buffer (pH 7.0). To estimate, the diffusion coefficient (D) of hemin/TNT/GCE, the linear plot of I_p versus $t^{-1/2}$ was achieved by the comparison of a) to e) that results in straight lines as shown in Fig. S5B. The plot of slope vs.conc. of nitrite (mM) as shown in Fig. S5C.

The diffusion coefficient and catalytic rate constant value of nitrite and their values were calculated to be 2.30×10^{-6} cm^2.s^{-1}, 5.51×10^4 cm^3.mol^{-1}.s^{-1} at corresponding to hemin/TNT/GCE was discussed in Supporting Information.

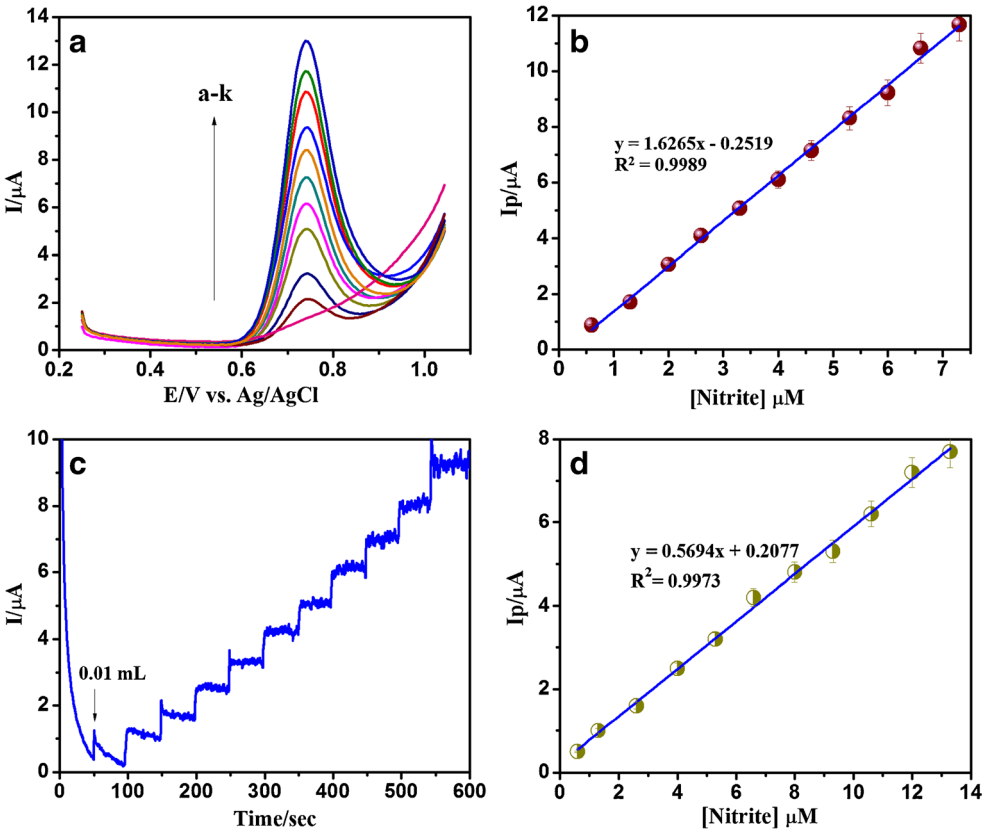

Fig. 4 DPV of hemin/TNT modified GCE in different concentrations of (0.6×10^{-6} M to 7.3×10^{-5} M) nitrite in buffer (pH 7.0) (**a**). Calibration plot of I_{pa} vs. conc. of nitrite (**b**). Amperometric response of hemin/TNT/GCE at an applied potential + 0.75 V subsequent addition of different concentrations ranges of (0.6×10^{-6} M to 13.3×10^{-5} M nitrite in buffer (pH 7.0) (**c**). Calibration plot of I_p vs. conc. of nitrite (**d**)

Electrochemical detection of nitrite

DPV method was employed to study the electrochemical detection of nitrite based on hemin/TNT/GCE as shown in Fig. 4a. It's more sensitive which eliminates the unwanted residual and charging currents. The electrochemical oxidation of nitrite was shown in the form of peak shaped different pulse voltammogram. Under the optimized experimental conditions, the oxidation peak current enhanced linearly with the increasing concentration of nitrite in the presence of buffer (pH 7.0). The peak currents were linearly proportional to nitrite concentrations in the range of 0.6×10^{-6} M to 7.3×10^{-5} M and the linear regression equation of $I_p(\mu M) = 1.6265\ C\ (\mu M) - 0.2519$ was accomplished with a correlation coefficient of 0.9989 as shown in Fig. 4b. The detection limit value (3σ/slope where σ = standard deviation) was found to be 84 nM at a signal to noise (S/N) ratio of 3. The prepared electrode shows good electrochemical sensitivity of 54.21 $\mu A \cdot \mu M^{-1} \cdot cm^{-2}$. The lowest LOD received with the present sensor, as compared to other reported methods (Table 1) evidenced that the modified GCE provided a good platform for the effective recognition of nitrite in water samples at low concentration ranges.

Amperometric studies

Amperometry strategy was utilized to measure the response of current for each addition of nitrite at different response time under hydrodynamic condition. A typical steady-state catalytic current-time response of hemin/TNT/GCE was investigated under constant stirring for step-wise injection of nitrite concentrations into the buffer (pH 7.0) and the applied potential was fixed at + 0.75 V vs. Ag/AgCl. Each addition of nitrite at 50 s intervals results a drastic raise in current response and then steady-state current value was reached within 5 s. Such as fast current response implies that the hemin/TNT/GCE efficiently promoted the oxidation of nitrite, is suitable for the real sample analysis. The (i-t) current response for the electrochemical oxidation of nitrite with different increment of nitrite concentration. The amperometric response was found to increase linearly with raise in the concentration ranges of 0.6 ×

Table 1 Comparative analysis on nitrite by analytical strategies

[a]Electrode	Method	Applied potential	LDR ($\mu molL^{-1}$)	R^2	LOD ($\mu molL^{-1}$)	Ref.
PEDOT/(CNCC/PDDA)/ GCE	AMP	+ 0.8	0.2 – 1.730	0.9984	0.057	[18]
PEDOT/AuNCs	AMP	+ 0.8	0.5 – 2600	0.997	0.017	[19]
PAOA/GCE	AMP	–	5 – 2000	0.9988	2	[7]
PANI-MoS_2/GCE	AMP	+ 0.9	4 – 4834	0.993	1	[23]
SiC Whisker electrode	AMP	+ 0.8	$5 \times 10^{-5} – 5 \times 10^{-5}$	0.9978	3.5	[5]
AgNPs/MWCNTs/GCE	DPV	–	0 – 1	0.999	0.095	[42]
SNPs/CPZ/Nf/GCE	DPV	–	20 – 120	0.9722	7	[43]
PtMWCNTs/GCE	AMP	+ 0.8	4.0×10^{-6} - 2.4×10^{-5}	0.9994	1.5	[44]
ACNTs/GCE	DPV	–	3.0 – 5.0	0.997	1.12	[45]
PtNWNs/GCE	AMP	+ 0.7	1 – 25	0.9927	0.14	[46]
PEDOT/PAS	AMP	+ 0.80	0.3 – 6594	0.9993	0.098	[25]
CoNS/GO/PPy/GCE	AMP	+ 0.80	0.001 – 3.167	0.998	0.0147	[26]
nHAp-PEDOT/GCE	AMP	+ 0.78	0.25 – 1045	0.9997	83	[27]
TiO_2/hemin/GCE	AMP	+ 0.75	$0.6 \times 10^{-6} – 13.3 \times 10^{-5}$	0.9983	0.059	This work

PEDOT/(CNCC/PDDA) - carboxylated nanocrystalline cellulose and poly (diallyl dimethyl ammonium) ions in a poly (3,4-ethlenedioxythiophene)

PEDOT/AuNCs - Gold nanoclusters doped poly (3,4-ethylenedioxythiophene) for highly sensitive electrochemical sensing of nitrite

PAOA/GCE - poly(aniline-*co*-*o*-aminophenol)-modified glassy carbon electrode

SiC - Silicon carbide and ACNT - Aligned carbon nanotubes

AgNPs/MWCNTs - Ag nanoparticles decorated multi walled carbon nanotubes

SNPs/CPZ/Nf - Silica nanoparticles / Chloropromazine /Nafion nanocomposites

PANI-MoS_2- polyaniline/molybdenum sulfide nanocomposite

PtMWCNTs - Platinum modified multiwalled carbon nanotubes

PtNWNs/GCE – Platinum nanowire network

PEDOT/PAS – poly(3,4-ethylenedioxythiophene)/polyacenic semiconductor

CoNS/GO/PPy/GCE – cobalt nanostructure/graphene oxide/polypyrrole

nHAp-PEDOT/GCE – nano-sized hydroxyapatite/poly(poly(3,4-ethylenedioxythiophene)

Table 2 Determination of nitrite in water samples ($n = 3$)

Sample	Added (μM)	Found (μM)	Recovery (%)	RSD (%)
Tape water	1	0.97 ± 0.08	97	0.9
	3	2.95 ± 0.25	98.3	1.5
	5	5.05 ± 0.47	101	2.6
Lake water	2	1.96 ± 0.19	98	1.4
	4	4.03 ± 0.32	100.7	2.5
	8	8.2 ± 1.08	102.5	3.0

10^{-6} M to 13×10^{-5} M of nitrite as shown in Fig. 4c. From the Fig. 4d, the linear regression equation is I_p (μM) = 0.5694 C (μM) + 0.2077 was accomplished with a correlation coefficient of 0.9973. The LOD was found to be 59 nM based on a ratio of signal-to-noise with the electrochemical sensitivity of 18.98 $\mu A\cdot\mu M^{-1}\cdot cm^{-2}$. The lowest LOD was procured with the present sensor when compared with other electrochemical sensors reported in the literature as shown in Table 1. From the table, the results evidently confirmed that the hemin/TNT/GCE can be used for the detection of nitrite in low concentration with improved sensitivity and fast response time.

Reproducibility, repeatability and interference

The repeatability of hemin/TNT/GCE in the determination of nitrite was investigated by performing five different electrode determined in same nitrite concentrations. The relative standard deviation (RSD) for the electrode response towards 3.3×10^{-6} M of nitrite was 1.74 %. To estimate the reproducibility of the response, a nitrite sensor, five electrodes were prepared of the same group and they were evaluated by performing the detection of 3.3×10^{-6} M of nitrite solution. The relative standard deviation (RSD) for the response of electrodes was below 3 %. These results showed the repeatability and reproducibility of the sensor for the detection of nitrite ion is in acceptable range. In addition, the storage stability of the prepared sensor was evaluated. For determination of 3.3×10^{-6} M of nitrite, there were no major decreases in the current response for the first 10 days. After that 5% decrease in current response was noted after storing for month duration. About 90 % current response is retained after 60 to 70 days. Hence, the long-term storage stability of the considered electrode was good enough for continuous operation.

The effect of interfering species on the determination of 6.6×10^{-6} M nitrite was examined by adding different interfering compounds into the electrochemical system using the common acid radical ions such as NaH_2PO_4, Na_2SO_3, sodium nitrate and NH_4F shows that only the spiking of nitrite generate current response and the others failed to induce the current signal at 100 times higher concentrations than that of nitrite (Fig. 5). Furthermore, Some redox active substance including biological molecules, polyphenols and flavonoids such as dopamine, folic acid, ascorbic acid, catechol, ellagic acid, quercetin, rutin, eugenol, caffeic acid and acetaminophen produced almost no interference at a 50-fold concentrations. We also investigated the influences of some environmental pollutants and saccharides such as hydrazine, H_2O_2, phenyl hydrazine, sucrose, glucose (30-fold concentrations relative to nitrite), did not disturb the current signal of nitrite and almost same magnitudes of current response were reproduced. From the above results it is inferred that the prepared sensor showed an excellent long-term storage stability and interference for

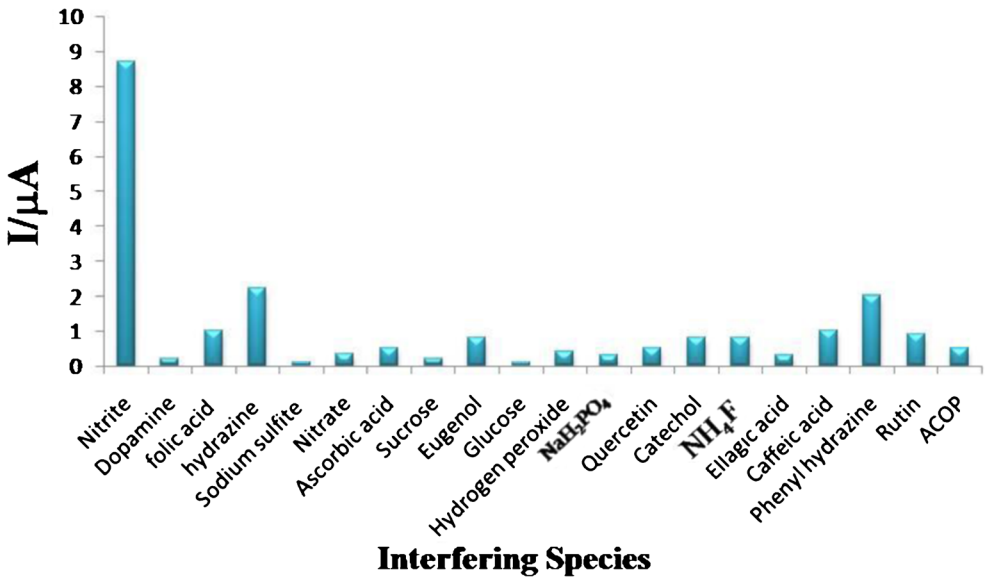

Fig. 5 Amperometric response of TNT/hemin/GCE upon successive addition of 6.6×10^{-6} M of nitrite and other interfering chemicals to 0.1 M buffer (pH 7.0) under hydrodynamic condition at the applied potential of + 0.75 V for modified GCE

the successful utilization of electrochemical determination of nitrite in water samples.

Real sample analysis

In order to investigate the practical application of the prepared system, the hemin/TNT/GCE based electrochemical sensor was applied to analyze nitrite levels in real sample like tap and lake water. The samples consisting of different concentrations of spiked nitrite were quantitatively analyzed using a standard addition method. The real samples were filtered using a 0.2 μm filter to remove unwanted micron sized particles. The results showed that the prepared electrode was highly selective and sensitive to nitrite. The procured results yield a good recovery in tap and lake water which were observed as 101%, and 102.4% for the 5 μM nitrite samples spiked, respectively as shown in Table 2.

The RSD values for the tested real samples were less than 3% and they were within the acceptable range. These consequences indicate that the prepared sensor showed an excellent determination of nitrites in real samples such as tape and lake waters.

Conclusion

A stable hemin functionalized titanium oxide nanotube based device was fabricated for the electrochemical detection of nitrite at pH 7.0. Here, we have prepared a hemin functionalized TNT exhibiting an enhanced oxidation peak current and CV results shows that they have good sensitivity towards nitrite ion. The TNT based nitrite sensors showed a high sensitivity and rapid response at room temperature than other electrochemical sensors reported in the literature. A novel and effective electrochemical sensing platform based on hemin/TNT modified GCE for sensitive and selective detection of NO_2^- by DPV and amperometry methods was accomplished. The novel device exhibited excellent electrochemical properties like low detection limit, good reproducibility and high stability towards the oxidation of nitrite. The present electrochemical sensing platform can be applied to monitor the level of nitrite in various water sources.

Acknowledgements The authors are grateful to Prof. A. Nirmala Grace, Director, and Centre for nanotechnology, VIT, Vellore for providing Raman data. One of the authors (Dr. K. P) thanks Prof. M.V. Sankaranarayanan and M. V. Beena, Department of Chemistry, IIT Madras, Chennai for providing the instrumental facility for EIS as well as amperometry analysis (CHI electrochemical workstation, 660B, USA).

Compliance with ethical standards

The author(s) declare that they have no competing interests.

References

1. Uzer A, Saglam S, Can Z, Erçag E, Apak R (2016) Electrochemical determination of food preservative nitrite with gold nanoparticles/p-aminothiophenol modified gold electrode. Int J Mol Sci 17(1253): 1–17. https://doi.org/10.3390/ijms17081253
2. Silva SM, Mazo LH (1998) Differential pulse voltammetric determination of nitrite with gold ultramicroelectrode. Electroanalysis 10:1200–1203. https://doi.org/10.1002/(SICI)1521-4109(199811)10:17<1200::AID-ELAN1200>3.0.CO;2-5
3. Li Y, Wang H, Liu X, Guo L, Ji X, Wang L, Tian D, Yang X (2014) Nonenzymatic nitrite sensor based on a titanium dioxide nanoparticles/ionic liquid composite electrode. J Electroanal Chem 719:35–40. https://doi.org/10.1016/j.jelechem.2014.02.006
4. Marlinda AR, Pandikumar A, Yusoff N, Huang NM, Lim HN (2015) Electrochemical sensing of nitrite using a glassy carbon electrode modified with reduced functionalized graphene oxide decorated with flower like zinc-oxide. Microchim Acta 182:1113–1122. https://doi.org/10.1007/s00604-014-1436-x
5. Dong H, Fang Z, Yang T, Yu Y, Wang D, Chou KC, Hou X (2016) Single crystalline 3C-SiC whiskers used for electrochemical detection of nitrite under neutral condition. Ionics 22:1493–1500. https://doi.org/10.1007/s11581-016-1666-5
6. Ma X, Miao T, Zhu W, Gao X, Wang C, Zhao C, Ma H (2014) Electrochemical detection of nitrite based on glassy carbon electrode modified with gold-polyaniline-graphene nanocomposites. RSC Adv 4:57842–57849. https://doi.org/10.1039/C4RA08543D.
7. Liu L, Cui H, An H, Zhai J, Pan Y (2017) Electrochemical detection of aqueous nitrite based on poly (aniline-*co*-*o*-aminophenol)-modified glassy carbon electrode. Ionics 23:1517–1523. https://doi.org/10.1007/s11581-017-1972-6
8. Ito K, Takayama Y, Makabe N, Mitsui R, Hirokawa T (2015) Ion chromatography for determination of nitrite and nitrate in seawater using monolithic ODS columns. J Chromatogr A 1083:63–67. https://doi.org/10.1016/j.chroma.2005.05.073
9. Wang G, Satake M (1996) Spectrophotometric determination of nitrite in environmental waters using column preconcentration on biphenyl. Microchim Acta 124:241–250. https://doi.org/10.1007/s00604-017-2180-9.
10. Cox RD, Frank CW (1982) Determination of nitrate and nitrite in blood and urine by chemiluminescence. J Anal Toxicol 6(3):148–152. https://doi.org/10.1093/jat/6.3.148
11. Liu QH, Yan XL, Guo JC, Wang DH, Li L, Yan FY, Chen LG (2009) Spectrofluorimetric determination of trace nitrite with a novel fluorescent probe. Spectrochim Acta 73(5):789–793. https://doi.org/10.1016/j.saa.2009.03.018
12. Zhuang Z, Lin H, Zhang X, Qiu F, Yang H (2016) A glassy carbon electrode modified with carbon dots and gold nanoparticles for enhanced electrocatalytic oxidation and detection of nitrite. Microchim Acta 183:2807–2814. https://doi.org/10.1007/s00604-016-1931-3.
13. Dai J, Deng D, Yuan Y, Zhang J, Deng F, He S (2016) Amperometric nitrite sensor based on a glassy carbon electrode modified with multi-walled carbon nanotubes and poly(toluidine blue). Microchim Acta 183:1553–1561. https://doi.org/10.1007/s00604-016-1773-z.
14. Zhou L, Wang JP, Gai L, Li DJ, Li YB (2013) An amperometric sensor based on ionic liquid and carbon nanotube modified composite electode for the determination of nitrite in milk. Sensors Actuators B 181:65–70. https://doi.org/10.1016/j.snb.2013.02.041
15. Cui L, Zhu J, Meng X, Yin H, Pan X, Ai S (2012) Controlled chitosan coated Prussian blue nanoparticles with the mixture of graphene nanosheets and carbon nanospheres as a redox mediator for the electrochemical oxidation of nitrite. Sensors Actuators B Chem 161:641–647. https://doi.org/10.1016/j.snb.2011.10.083

16. Lin CY, Balamurugan A, Lai YH, Ho KC (2010) A novel poly (3, 4-ethylenedioxythiophene)/ iron phthalocyanine/ multi-wall carbon nanotubes nanocomposite with high electrocatalytic activity for nitrite oxidation. Talanta 82:1905–1911. https://doi.org/10.1016/j.talanta.2010.08.010
17. Jiao S, Jin J, Wang L (2015) One-pot preparation of Au-RGO/PDDA nanocomposites and their application for nitrite sensing. Sensors Actuators B 208:36–42. https://doi.org/10.1016/j.snb.2014.11.020
18. Xu GY, Liang SP, Fan JS, Sheng G, Luo XL (2016) Amperometric sensing of nitrite using a glassy carbon electrode modified with a multilayer consisting of carboxylated nanocrystalline cellulose and poly(dialyldimethyl ammonium) ions in a PEDOT host. Microchim Acta 183:2031–2037. https://doi.org/10.1007/s00604-016-1842-3
19. Fan X, Lin P, Liang S, Hui N, Zhang R, Feng J, Xu G (2017) Gold nanoclusters doped poly(3,4-ethylenedioxythiophene) for highly sensitive electrochemical sensing of nitrite. Ionics 23:997–1003. https://doi.org/10.1007/s11581-016-1865-0
20. Zhao K, Song H, Zhuang S, Dai L, He P, Fang Y (2007) Determination of nitrite with the electrocatalytic property to the oxidation of nitrite on thionine modified aligned carbon nanotubes. Electrochem Commun 9:65–70. https://doi.org/10.1016/j.elecom.2006.07.001
21. Mani V, Periasamy AP, Chen SM (2012) Highly selective amperometric nitrite sensor based on chemically reduced graphene oxide modified electrode. Electrochem Commun 17:75–78. https://doi.org/10.1016/j.elecom.2012.02.009
22. Deng K, Zhou J, Huang H, Ling Y, Li C (2016) Electrochemical determination of nitrite using a reduced graphene oxide–multiwalled carbon nanotube-modified glassy carbon electrode. Anal Lett 49:2917–2930. https://doi.org/10.1080/00032719.2016.1163364.
23. Zhang Y, Chen P, Wen F, Huang C, Wang H (2016) Construction of polyaniline/molybdenum sulfide nanocomposite: characterization and its electrocatalytic performance on nitrite. Ionics 22:1095–1102. https://doi.org/10.1007/s11581-015-1634-5.
24. Rabti A, Ben Aoun S, Raouafi N (2016) A sensitive nitrite sensor using an electrode consisting of reduced graphene oxide functionalized with ferrocene. Microchim Acta 183:3111–3117. https://doi.org/10.1007/s00604-016-1959-4
25. Chen L, Liu X, Wang C, Lv S, Chen C (2017) Amperometric nitrite sensor based on a glassy carbon electrode modified with electrodeposited poly(3,4-ethylenedioxythiophene) doped with a polyacenic semiconductor. Microchim Acta 184:2073–2079. https://doi.org/10.1007/s00604-017-2189-0.
26. Wang J, Hui N (2017) A nanocomposite consisting of flower-like cobalt nanostructures, graphene oxide and polypyrrole for amperometric sensing of nitrite. Microchim Acta 184:2411–2418. https://doi.org/10.1007/s00604-017-2247-7
27. Wang G, Han R, Feng X, Li Y, Lin J, Luo X (2017) A glassy carbon electrode modified with poly(3,4-ethylenedioxythiophene) doped with nano-sized hydroxyapatite for Amperometric determination of nitrite. Microchim Acta 184:1721–1727. https://doi.org/10.1007/s00604-017-2180-9
28. Kasuga T, Hiramatsu M, Hoson A, Sekino T, Niihara K (1998) Formation of titanium oxide nanotube. Langmuir 14:3160–3163. https://doi.org/10.1021/la9713816.
29. Kafi AKM, Wu G, Chen A (2008) A novel hydrogen peroxide biosensor based on the immobilization of horseradish peroxidase onto Au-modified titanium dioxide nanotube arrays. Biosens Bioelectron 24:566–571. https://doi.org/10.1016/.j.bios.2008.06.004
30. Furjan MSHA, Cheng K, Weng W, Ni J (2017) Improvement in sensing performance of H_2O_2 biosensor electrode through modification of anatase TiO_2 nanorods and pretreatment of electrochemical reduction. Sensors Mater 29: 95–103. https://doi.org/10.18494/SAM.2017.1418
31. Ghadiri E, Taghavinia N, Zakeeruddin SM, Gratzel M, Moser JE (2010) Enhanced electron collection efficiency in dye-sensitized solar cells based on nanostructured TiO_2 hollow fibers. Nano Lett 10:1632–1638. https://doi.org/10.1021/nl904125q.
32. Shingubara S, Kagamiyama H (2003) Fabrication of nanomaterials using porous alumina templates. J Nanopart Res 5:17–30. https://doi.org/10.1023/A:1024479827507
33. Shimizu K, Imai H, Hirashima H, Tsukuma K (1999) Low temperature synthesis of anatase thin films on glass and organic substrates by direct deposition from aqueous solutions. Thin Solid Films 351:220–224. https://doi.org/10.1016/S0040-6090(99)00084-x.
34. Yang J, Mei S, Ferreira JMF, Norby P, Quaresma S (2005) Fabrication of rutile rod like particle by hydrothermal method: an insight into HNO_3 peptization. J Colloid Interface Sci 283:102–106. https://doi.org/10.1016/j.jcis2004.08.109
35. Imai H, Matsuta M, Shimizu K, Hirashima H, Negishi N (2002) Morphology transcription with TiO_2 using chemical solution growth and its application for photocatalysts. Solid State Ionics 151:183–187. https://doi.org/10.1016/s0167-2738(02)00708-7
36. Alexander M, Pandian K (2013) Linen fiber template-assisted preparation of TiO_2 nanotubes: Palladium nanoparticle coating and electrochemical applications. J Solid State Electrochem 17:1117–1125. https://doi.org/10.1007/s10008-012-1981-3
37. Ederozey AMM, Akil HM, Azhar AB, Ariffin MIZ (2007) Chemical modification of kenaf fibers. Mater Lett 61:2023–2025. https://doi.org/10.1016/j.matlet.2006.08.006
38. Ochi S (2008) Mechanical properties of kenaf fibers and kenaf/PLA composites. Mech Mater 40:446–452. https://doi.org/10.1016/j.mechmat.2007.10.006
39. Guo Y, Deng L, Li J, Guo S, Wang E, Dong S (2011) Hemin-graphene hybrid nanosheets with intrinsic peroxidase like activity for label-free colorimetric detection of single nucleotide polymorphism. ACS Nano 5:1282–1290. https://doi.org/10.1021/nm1029586.
40. Peteu SF, Whitman BW, Galligan JJ, Swain GM (2016) Electrochemical detection of peroxynitrite using hemin-PEDOT functionalized boron-doped diamond microelectrode. Analyst 141:1796–1806. https://doi.org/10.1039/C5AN02587G
41. Wu X, Chai Y, Yuan R, Chen S, Zhang M, Zhang J (2013) Hemin functionalized multiwalled carbon nanotubes as a matrix for sensitive electrogenerated chemiluminescence cholesterol biosensor. Electroanalysis 25:2700–2706. https://doi.org/10.1002/elan.201300311
42. Wan Y, Zheng YF, Wan HT, Yin HY, Song XC (2017) A novel electrochemical sensor based on Ag nanoparticles decorated multi-walled carbon nanotubes for applied determination of nitrite. Food Control 73:1507–1513. https://doi.org/10.1016/j.foodcont.2016.11.014.
43. Amini N, Shamsipur M, Golivand MB, Naderi K (2017) Electrocatalytic and new electrochemical properties of chloropromazine in to silica NPs/ Chloropromazine/ Nafionnanocomposite: application to nitrite detection at low potential. Microchim Acta 131:43–50. https://doi.org/10.1016/j.micro.2016.11.006
44. Etesami M, Mohamed N (2016) Preparation of Pt/MWCNTs catalyst by Taguchi method for electrooxidation of nitrite. J Anal Chem 71:185–194. https://doi.org/10.1134/S1061934816020040
45. Wang X, Cao T, Zuo Q, Wu S, Uchiyama S, Matsuura H (2016) Sensitive nitrite detection using a simple electrochemically aminated glassy carbon electrode. Anal Methods 8:3445–3449. https://doi.org/10.1039/C6AY00015K
46. Chen SS, Shi YC, Wang AJ, Lin XX, Feng JJ (2017) Free-standing platinum nanowire networks with clean surface: Highly sensitive electrochemical detection of nitrite. J Electroanal Chem 791:131–137. https://doi.org/10.1016/j.jelechem.2017.03.016.